High-Performance Optical Power Limiting Filters at Telecommunication Wavelengths: When Aza-BODIPY Dyes Bond to Sol-Gel Materials

Sylvain David, D. Chateau, H.-J. Chang, L.H. Karlsson, M.V. Bondar, C. Lopes, Boris Le Guennic, D. Jacquemin, G. Berginc, Olivier Maury, et al.

High performance optical power limiting filters at telecommunication wavelengths: when aza-BODIPY dyes bond to sol-gel materials.

Sylvain David,[a,£] Denis Chateau,[a,£] Hao-Jung Chang,[b] Linda H Karlsson,[c] Mykhailo V. Bondar,[d] Cesar Lopes,[c] Boris Le Guennic,[e] Denis Jacquemin,[f] Gérard Berginc,[g] Olivier Maury,[a,*] [b] Stéphane Parola,[a,*] Chantal Andraud [a,*]

a. Dr. S. David, Dr. D. Chateau, Dr. O. Maury, Prof. S. Parola, Dr. C. Andraud; Univ. Lyon, ENS Lyon, CNRS, Université Lyon 1, Laboratoire de Chimie, UMR 5182, 46 Allée d'Italie, 69364 Lyon, France

b. H.-J. Chang, CREOL, The College of Optics and Photonics, University of Central Florida, Orlando, FL 32816, USA

c. Dr. L.H. Karlsson, Dr. C. Lopes; Electro-optical Systems, Swedish Defense Research Agency (FOI) Linköping SE-581 11, Sweden.

d. Dr. M. V. Bondar, Institute of Physics NASU, Prospect Nauki, 46, Kyiv-28, 03028, Ukraine

e. Dr. B. Le Guennic; Univ. Rennes, CNRS, ISCR (Institut des Sciences Chimiques de Rennes) UMR 6226, 35000 Rennes, France

f. Prof. D. Jacquemin; CEISAM UMR 6230, CNRS, Université de Nantes, F-44000 Nantes, France.

g. Dr. G. Berginc; Thales LAS France, 2 Avenue Gay Lussac, 78990 Élancourt, France

KEYWORDS: Optical limiting; nonlinear-optics; Aza-BODIPY dyes; two-photon absorption; sol-gel material.

ABSTRACT: An optical power limiter (OPL) device can change its optical properties depending on the input light intensity: it is ideally transparent at low incident power and presents a decrease in transmission when the incident intensity increases. This phenomenon can be used for protection of optical sensors. This paper presents the design of a functionalized aza-BODIPY chromophore, combining good nonlinear two-photon absorption and exited state absorption in the short wave infra-red range (1300-1600 nm). The aza-BODIPY chromophores also show excellent thermal and photochemical stabilities. Their covalent grafting to a sol-gel matrix lead to the formation of class-II sol-gel materials that allows for extraordinary doping concentrations of up to 280 mol.L^{-1} (40 wt%), which results in highly efficient OPL performances at 1550 nm.

An optical power limiting (OPL) filter has the capability of modifying its global transmittance depending on the input light intensity.[1-3] Nowadays, the tremendous development of eye-safe LIDAR (LIght Detection And Ranging) systems working at telecommunication wavelengths (1550 nm), for applications in aeronautics (telemetry), but also in defense (active imaging) and civilian transportation (autonomous vehicles guiding systems) triggered a rapidly growing demand for efficient OPL devices at this wavelength, but more generally in the SWIR (Short Wave Infra-Red) band. For field applications, the OPL filter should fulfill a set of requirements: (i) a broad spectral efficiency in the spectral range-of-interest (ROI = 1300-1600 nm), (ii) a high transmission in the off-state at low incident light intensity (minimum 85%), (iii) a low transmission in the on-state at high incident light intensity (below the damage threshold of the optical detector), (iv) a very fast response time and (v) a good environmental stability in order to be adapted to existing optical devices.[3]

As a general point of view, the OPL process can be driven by nonlinear optical phenomena,[3-4] such as nonlinear refraction,[5-7] nonlinear scattering,[8-9] reverse saturable absorption[10-13] and, two- (multi)-photon absorption (2PA). Consequetly, the process is triggered by the incident light itself, which induces an instantaneous nonlinear response within the material (sub-fs timescale). This self-activated instantaneous response is a key advantage for practical applications. It has been widely demonstrated that OPL in the visible spectral range can be strongly enhanced if an excited-state absorption (ESA) phenomenon overlaps temporally and spectrally with the 2PA.[3, 10, 14-18] However, in spite of the rapid development since 2005 of two-photon dyes absorbing in the SWIR spectral range,[19-24] OPL at 1300-1600 nm is a field of research still in its infancy. Therefore, few reports describing OPL

experiments at telecommunication wavelengths have appeared; so far, polymethine dyes,[25-26] functionalized porphyrins[27] and aza-BODIPY dyes in a solvent solution have been presented.[28-29] In all cases, a 2PA induced ESA photophysical process is responsible for the OPL mechanism.[30] However, if solid-state materials operating in the visible wavelengths are well-known,[31] up to now, only one solid-state material for OPL in the SWIR has been described in the litterature.[32] This material, reported by our group is a sol-gel glass doped with the functionalized aza-BODIPY chromophore **1** (**Erreur ! Source du renvoi introuvable.**).[32] Despite the encouraging results obtained with this first material, the OPL response remained far from the technical requirements for practical use in real optical systems. In particular, the dye loading, which is one of the key parameters for improving the OPL properties was limited to 8 wt% (approx. 85 mM), consequently limiting the performances. This limitation is explained by the poor compatibility between the dyes and the matrix in such host-guest approach, where the matrix-dye interface strength is weak. Above this concentration the gel, during its contraction, expelled the dye. An aggregation of the dye inside the matrix is also observed which causes a drop in the linear transmission.

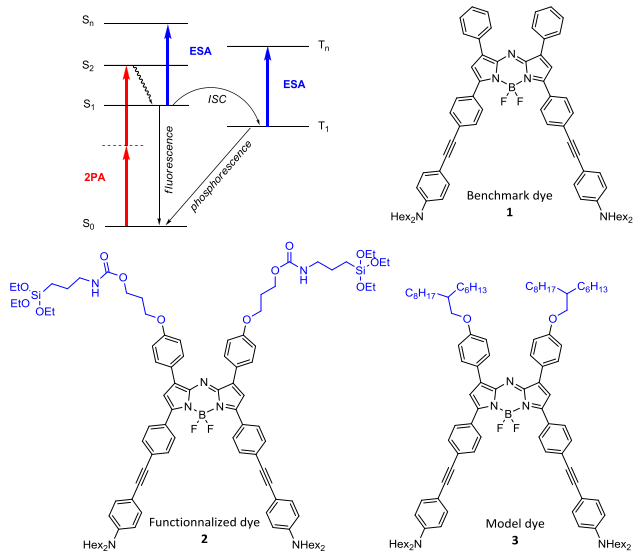

Figure 1. Perrin-Jablonski diagram with the different photophysical processes involved in a molecular based OPL. Structure of the benchmark dye **1** and the functionalized and model chromophores **2** and **3**.

In order to prevent such phase segregation during the process, an alternative strategy is known, increasing the interface strength through covalent bonding between the hybrid matrix and the molecular host, here the dye.[33] In contrast to weak interaction systems, named Class-I sol-gel materials, where the guest dye is only dispersed in the matrix, Class-II refers to materials where the dye is covalently grafted to the host matrix. Such alternative has been previously investigated for OPL hybrid materials in the visible range. It brought improvements but in most cases with still limited optical performances.[15, 34-37] These results led us to turn to the so-called class-II sol-gel hybrid materials with covalent interactions between matrix and molecular host. This process usually permits to achieve high doping concentrations without separation of the dye.[15] However, in some cases, the rigidifying of the dye structure induced by the grafting on the matrix can be counter-productive, as the solid-state constraints disrups the conjugated skeleton hence reducing the nonlinear optical properties.[38] Class-II materials for OPL applications in the visible range have been reported using platinum acetylide complexes as the nonlinear doping chromophore. A high concentration was achieved (*i.e.* 120 mM) without any perturbation of the optical properties of the dye.[15] This procedure was therefore extended to aza-BODIPY dye. **1** was functionalized with triethoxysilane moieties, through the alkoxy-functionalization of upper 1,7 positions (molecule **2**, Erreur ! Source du renvoi introuvable.). The effect of such alkoxy-donating group functionalization on the photophysical properties of the dye was thoroughly investigated on the model chromophore **3** and compared to **1** both theoretically and experimentally. Finally, class-II materials with improved doping ratio were prepared for OPL properties studies.

The synthesis of compounds **2** and **3** follows the classical route for symmetrical aza-BODIPY dyes, as already described for the benchmark compound **1** (Schemes S1 and S2).[28] In the case of **2**, an intermediate aza-BODIPY featuring hydroxyl-propanol (-O-$(CH_2)_3$-OH) group at the top positions is prepared and the tri-ethoxysilane reactive function was introduced at the last step by reaction with 3-(triethoxysilyl)propyl isocyanate in the presence of dibutyltindilaurate as catalyst. Synthetic details and complete characterization are given in the Supporting Information (SI).

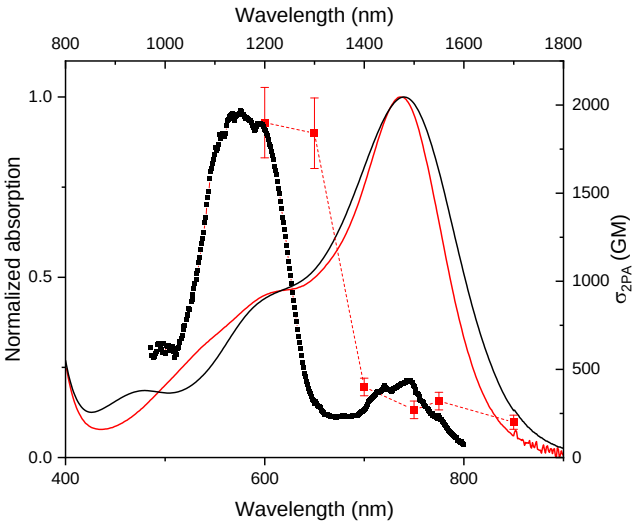

Figure 2. Comparison of the linear and nonlinear two-photon absorption of **1** (black) and **3** (red) in DCM solution. Two-photon absorption spectra of **1** and **3** were measured by two-photon excited fluorescence in CCl_4 (▪) and open-aperture Z-scan measurements in DCM (▪), respectively.

Due to the moister sensitivity of the triethoxysilane group in molecule **2**, all photophysical measurements were performed in DCM on the model compound **3** which has simple alkoxy substituents (**Erreur ! Source du renvoi introuvable.** and Table 1). The measurements, performed in dichloromethane (DCM) solution, were compared with the reference dye **1**. Both benchmark dye **1** and molecule **3** show a very similar linear absorption spectrum with

respective absorption maxima in DCM at 740 and 736 nm and a slight narrowing of the lower energy transition for **3**. The second transition in the 500-600 nm region is slightly modified as well. If the shoulder at ca. 600 nm, attributed to a transition having mainly Charge Transfer (CT) character in the benchmark chromophore is identical for the dye **3**, it seems that a second band around 525 nm superimposes with the latter band, causing the broadening of the spectrum. All these minor modifications in linear absorption indicate that upper alkoxy donating groups have weak impact on the electronic transitions. In addition, both compounds are not emissive in DCM[29] though the emission can be restored in apolar solvents such as toluene (Figure S1). The emission profiles are almost identical but dye **3** exhibits an improved quantum yield and a longer lifetime (Table 1).

Table 1. Linear and nonlinear optical properties of **1** and **3** in dichloromethane. λ_{max} and λ_{em} are the maximal absorption and emission wavelength, ε the extinction coefficient, ϕ and τ the radiative quantum yield and lifetime, σ_{2PA} and σ_{ESA} the 2PA and ESA cross-sections at 1550 nm.

Molecule	**1**	**3**
λ_{max} [nm]	740	736
ε [$M^{-1}.cm^{-1}$]	57000	65000
λ_{em}[a] [nm]	826	804
ϕ[a,b]	0.04	0.11
τ[a] [ns]	0.7	1.4
$\sigma_{2PA@1550\ nm}$ [GM]	236[c]	320 ± 50[e]
$\sigma_{ESA@1550\ nm}$ [10^{-16} cm^2]	0.84[d]	1.75[e]

a) in toluene; b) using aza-BODIPY dyes as a reference[39] (ϕ = 0.36 in $CHCl_3$); c) using TPEF in CCl_4;[29] d) using pump-probe experiment in DCM;[29] e) using Z-scan measurements in DCM.

To obtain more insights into the excited states involved in electronic transitions of these dyes, we performed first principle calculations, using an approach validated previously for a similar class of dyes[29, 40] (see the SI for details). To make these calculations feasible, the long alkyl chains of the dihexylamino and decylhexylalcoxy fragments have been replaced by methyl groups (simplified dyes **1**th and **3**th, respectively depicted Figure S3) and the main results are displayed in Figure 3 and Table 2. The lowest energy transition S_o-S_1, was calculated at 611 and 610 nm respectively for **1**th and **3**th. The fact that the computed absorption wavelength is significantly smaller than the experimental value is the logical consequence of the neglect of vibronic couplings and the cyanine nature of the transition where the electronic density changes are mainly localized on the aza-BODIPY core, the peripheral groups at the top or the bottom of the molecule playing a minor role for both systems. As previously observed for **1**,[29] the excited state representations (Figure 3) show that the lowest transition is mainly localized on the aza-BODIPY core. There is nevertheless a small CT from the ethynyl groups towards the core.[29] Moderate values of transferred charge (q_{CT} 0.48 and 0.44 e) over a distance (d_{CT}) of 2.26 and 1.63 Å, for **1**th and **3**th respectively are in good agreement with this assumption. As a consequence, the calculated 2PA cross section are modest. In contrast, the three higher energy transitions S_o-S_i (i = 2, 3, and 4) present stronger CT character from the bottom donating group (for **1**th and **3**th) to the aza-BODIPY core, with an additional short-range contribution of the top substituent for **3**th in the case of S_o-S_2. As expected, all these transitions present larger q_{CT} values spread over a longer d_{CT} distance compare to S_o-S_1 (Table 2) and do contribute more efficiently to the 2PA cross-section.

Table 2. Theoretical (vertical) absorption wavelength (λ), one-photon absorption oscillator strength (*f*), CT distance and charge (d_{CT} and q_{CT}), as well as 2PA cross-section (σ_{2PA}) for the four lowest-lying states of the simplified dyes **1**th and **3**th.

dyes	S_o-S_i	**λ [nm]**	***f*** **(1PA)**	$\mathbf{d_{CT}}$ **[Å]**	$\mathbf{q_{CT}}$ **[e]**	$\boldsymbol{\sigma_{2PA}}$ **[GM]**
1th	S_1	611	1.02	2.26	0.48	175
	S_2	431	0.99	4.37	1.08	3760
	S_3	417	0.01	0.60	0.68	1160
	S_4	394	0.00	3.90	0.88	1340
3th	S_1	610	1.06	1.63	0.44	95
	S_2	447	0.02	1.41	0.69	1030
	S_3	430	1.29	1.96	0.79	1850
	S_4	403	0.03	2.58	0.78	3410

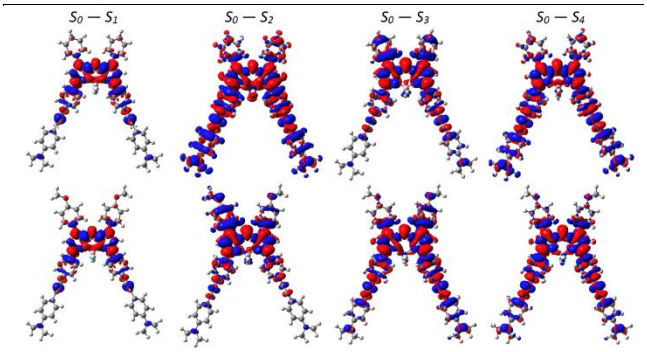

Figure 3. Electron density difference plots for the four lowest-lying excited states of **1**th (top) and **3**th (bottom). The red (blue) zones represent regions of increase (decrease) of the density upon electronic transition. A contour threshold of 8 10^{-4} au is used.

The 2PA properties of **3** were determined by open aperture Z-scan in DCM solutions using a fs-optical parametric amplifier pumped by a Ti:Sapphire source with a typical pulse duration of 150 fs (Table 1). The experimental nonlinear transmittance curve obtained (Figure S2) was fitted using the complete propagation equation (eq 1) taking into account both 2PA and ESA phenomena,

$$\frac{dI}{dz} = -\alpha_2 I^2 - \sigma_{ESA} N_e I \quad (1)$$

where I represents the light irradiance, z the propagation axis, α_2 the 2PA coefficient, σ_{ESA} the ESA cross section and N_e describes the first excited-state population after 2PA absorption. Using this model, both 2PA and ESA cross-sections could be determined simultaneously for a given wavelength using the following equation (2)

$$\sigma_{2PA} = \frac{\hbar\omega\alpha_2}{N} \quad (2)$$

where *N* represents the molecular density and ħω the photon energy at the operating wavelength. Typical Z-scans at 1550 nm for **3** and related fitting curves are depicted in Figure S2 leading to a 2PA cross section of 320 ± 50 GM and an ESA cross section of 1.75±0.3 10^{-16} cm² (see Table S1 for other wavelengths). These values are comparable with that obtained for the benchmark molecule **1** (σ_{2PA} = 236 GM and σ_{ESA} = 0.84 10^{-16} cm² in Table 1) keeping in mind that these latter data have been obtained using different and independent techniques, *i.e.* two-photon excited fluorescence and NIR pump-probe techniques for 2PA and ESA measurements, respectively.[29] Considering experimental uncertainties for both techniques, it appears that molecules **1** and **3** present comparable 2PA and ESA in the 1300-1600 nm range (Figure 2).

For both systems, the weak 2PA band overlaps with the intense linear "cyanine" type transition (Figure 2) in agreement with the calculated σ_{2PA} of 175 and 95 GM respectively for simplified molecules **1'** and **3'** (Table 2); the origin of nonlinear properties can be ascribed to the weak CT character of this absorption transition, as mentioned above. In addition, an intense 2PA band around 2000 GM, has been measured at higher energies matching with the shoulder of the linear absorption spectra, (Figure 2) corresponding to the overlap of the S_0-S_i (i = 2, 3, and 4) with stronger CT character. These experimental data are further corroborated by the high σ_{2PA} calculated values (Table 2) (3760 and 3410 GM) for S_0—S_2 and S_0—S_4 transitions of **1'** and **3'** respectively. It must be noted that, as previously observed,[29] calculations show for molecules **1**th and **3**th the existence of an intense 2PA transition corresponding to a forbidden 1PA transition (S_0-S_3 and S_0-S_4 for **1**th and S_0-S_2 and S_0-S_4 for **3**th, respectively). All these close energy transitions may contribute to the overall 2PA spectrum.

Finally, the thermal and photochemical stability of dye **3** was evaluated before incorporation into the matrix. Thermogravimetric analysis show a Td^{10} value of 375°C (Figure S4). This value is very high for an organic dye[41] and fully compatible with hybrid materials synthesis and practical application. On the other hand; the photochemical stability of **3** was evaluated in air-saturated DCM with the absorption method described previously in detail.[42] The photodecomposition quantum yield, ϕ_{ph}, of solutions of **3** at ≈ 635 nm, performed with a continuous wave (CW) diode laser with an average irradiance ≈ 500 mW/cm², was determined to 1.10^{-8}. This level of photostability is very high, comparable with the best laser dyes.[43-45]

Having checked that the model chromophore **3** fulfills all the molecular prerequisites for being used as the active dye in OPL materials, the synthesis of hybrid sol-gel materials containing molecule **2** featuring reactive triethoxysilane moieties was undertaken. The general synthesis protocol consisted in mixing compound **2** with a sol composed of a 1:1 mixture of VTMOS (vinyltrimethoxysilane) and MTEOS (methyltriethoxysilane). Modifications have been made compared to the previously published protocol[32] to account for class-II materials specificities. The overall hydrolysis-condensation kinetics were controlled by adding gelation agents like *N,N*-Dimethylaminopropyl-trimethoxysilane (DMATMS) and tetrabutylammonium fluoride (TBAF) in catalytic amounts. The catalyst amount was adapted to the quantity of dyes added to the sol-gel matrix. The condensation ratio of the prepared matrix is extremely high, leaving very few available silanols for the condensation of the added dyes with the silica network. This favorizes the dyes self-condensation and further aggregation and optical diffusion in the solid material. In order to provide available silanol groups for the reaction with the dyes, a low amount of water and fresh VTMOS monomer were added.

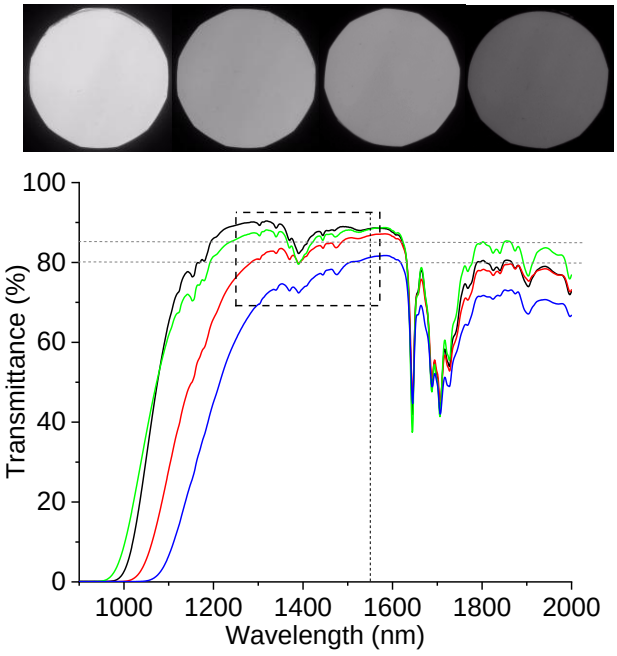

Figure 4. (Top) NIR picture of xerogel **MRef**, **M10**, **M20**, **M40**, after polishing (from left to right). The increased darkening is due to red-shift of the cut-off absorption wavelength of the dye with incremental concentration and also to the lower sensitivity of the camera over 1200 nm. All four images were taken with similar exposure. (bottom) Transmittance of materials **MRef** (black), **M10** (green), **M20** (red) and **M40** (blue) after polishing. Dotted box represents the ROI, horizontal dotted lines represent the transmittance at 80 and 85% and vertical dotted line is 1550 nm wavelength used for OPL experiments.

With this strategy, no dye aggregation or phase separation is observed during the preparation. The xerogel was readily obtained after drying at 45°C for 2 days as shiny dark disks (1.5 cm diameter, 2 mm thickness). The optical qualities of these materials were qualitatively estimated by a home-made device able to evaluate qualitatively their SWIR transparency and homogeneity (see the SI, Figure S5, S6 and Figure 4). The presence of TBAF was mandatory for obtaining xerogels with good optical quality (Figure S6).

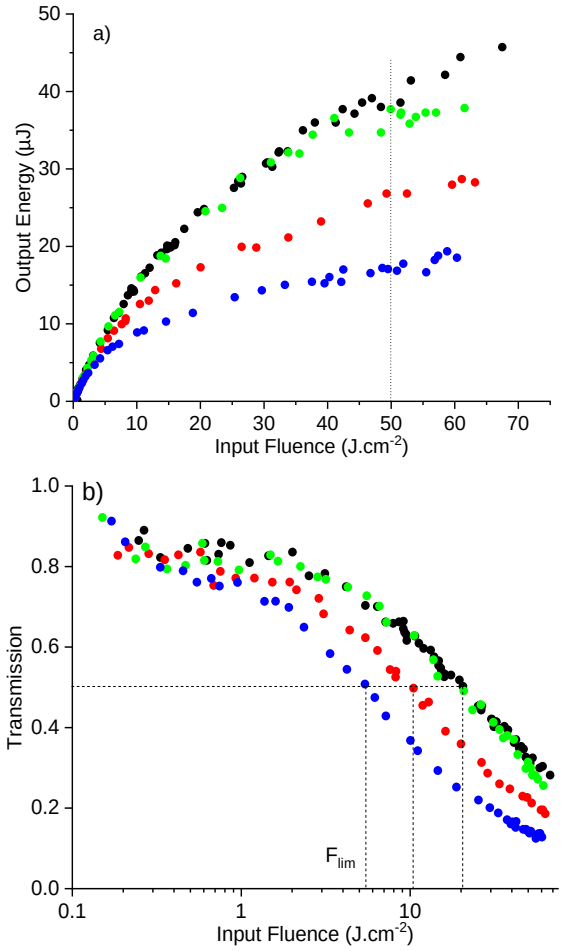

Figure 5. Optical limiting performances at 1550 nm for materials **M10** (●), **M20**(●), **M40**(●). For comparison, the reference doped material **MRef** (●) was measured under the same conditions. Two representations are proposed: (top) Out-put energy vs incident fluence and (bottom) transmittance vs incident fluence (in log scale). The F_{lim} thresholds are indicated by dotted lines.

This optimized protocol was used for the preparation of a series of xerogels (**M10**, **M20**, **M40**) containing increased concentration of aza-BODIPY dye **2** (10, 20 and 40 wt% corresponding to 70, 140 and 280 mol.L^{-1}, respectively, Table S1). As a reference, we used the already described **MRef** material,[32] with a 5 wt% doping concentration of dye **1** (approx. 56 mM). The final materials were mechanically polished, yielding 1 mm thick shiny black disks of optical quality and perfectly parallel faces. Interestingly, all studied materials are very homogeneous without any apparent defect (dark spots, cracks...Figure 4). In addition, transmittance spectra were measured and compared with reference host-guest material **MRef** (**Erreur ! Source du renvoi introuvable.**. Material **M10** has a transmittance very close to that of **MRef**. The increase in concentration caused a red-shift in cutoff wavelength on materials **M20** and **M40** corresponding to the red tail of the chromophore absorption. The linear transmission, in the 1600-1800 nm region, decreased due to matrix absorption. However, in the ROI (1300-1600 nm) and more particularly at 1550 nm, the wavelength of interest, all materials have an excellent transmission ranging from 81% to 88%, which matches the 85 % requirement.

The optical limiting experiments were performed at 1550 nm using 5 ns laser pulses and a f/5 system (see SI for description) and the experimental results are reported in Figure 5. Material **M10** shows a very similar OPL behavior as **MRef,** which agrees with the comparable dye concentration in both materials. As expected the OPL performance improves with an increase in doping concentration. In order to compare the materials OPL performances further, the limiting threshold, F_{lim}, defined as the fluence at which the transmittance reaches 50% is used. This value is 21 J.cm^{-2} for both materials **MRef** and **M10**, 10 J.cm^{-2} for **M20** and 5 J.cm^{-2} for **M40**. This indicates a 4-fold increase of the material performances compared to the reference. We also observe a two-fold decrease in F_{lim} with a two-fold increase in doping concentration. The linear stepwise increase of the OPL performances of these sol-gel materials therefore indicates that the nonlinear properties of the dye is not affected by an increase in concentration nor by the covalent bonding to the matrix. The materials were thoroughly inspected after the OPL experiments, under visible and IR light, and no trace of laser induced damages was observed for the applied experimental conditions. This is in accordance with the observed high photochemical stability of the materials.

In conclusion, this article describes the potential use of class-II sol-gel materials, containing substituted aza-BODIPY dyes, for OPL applications at telecommunication wavelengths. The presented preparation method allows for reaching high chromophore concentrations and avoiding aggregation issues, thanks to the covalent grafting of the chromophore to the matrix. More importantly is the fact that the nonlinear properties are preserved. The resulting xerogels are homogeneous with high linear transparency in the SWIR spectral range. Their remarkable mechanical properties allowed preparation of prototype with high optical quality after polishing. Finally, the materials showed a significant improvement of the OPL performances with the concentration increase. This is accompanied with a damage resistance to high fluence laser irradiation. The presented results, therefore, constitute a significant step towards high performance optical limiters for applications in SWIR.

ASSOCIATED CONTENT

Supporting Information. Synthetic procedure and chemical caracterisation of dyes **2** and **3**, sol gel material preparation protocols, complete description of the spectroscopy, imaging and OPL set-ups are described in the Supporting Information. This material is available free of charge via the Internet at http://pubs.acs.org."

AUTHOR INFORMATION

Corresponding Author

chantal.andraud@ens-lyon.fr
olivier.maury@ens-lyon.fr
stephane.parola@ens-lyon.fr

Author Contributions

£ both authors contribute equally to the work. The manuscript was written through contributions of all authors. All authors have given approval to the final version of the manuscript.

ACKNOWLEDGMENT

Authors acknowledge Drs. Eric Van Stryland and David Hagan and the CREOL Nonlinear Optics Laboratories for their collaboration and assistance for the determination of the two-photon cross-section. Authors thank Thales LAS for financial support and for the grant of SD. The Swedish Defence Research Agency (FOI) is also thanked for financial support. D.J. is indebted to the CCIPL computational center installed in Nantes for (very) generous allocation of cpu time. Hampus Lundén is acknowledged for his contribution regarding the OPL set-up.

ABBREVIATIONS

SWIR, short wavelength infra-red; OPL, optical power limiting; DCM, dichloromethane.

REFERENCES

1. Miller, M. J.; Mott, A. G.; Ketchel, B. P., *General optical limiting requirements*. SPIE: 1998; Vol. 3472.
2. W. Spangler, C., Recent development in the design of organic materials for optical power limiting. *J. Mater. Chem.* **1999,** *9* (9), 2013-2020.
3. Dini, D.; Calvete, M. J.; Hanack, M., Nonlinear Optical Materials for the Smart Filtering of Optical Radiation. *Chem. Rev.* **2016,** *116* (22), 13043-13233.
4. Tutt, L. W.; Boggess, T. F., A review of optical limiting mechanisms and devices using organics, fullerenes, semiconductors and other materials. *Prog. Quantum Electron.* **1993,** *17* (4), 299-338.
5. Leite, R. C. C.; Moore, R. S.; Whinnery, J. R., Low absorption measurements by means of a thermal lens effect using an He–Ne laser. *Appl. Phys. Lett.* **1964,** *5* (7), 141-143.
6. Leite, R. C. C.; Porto, S. P. S.; Damen, T. C., The Thermal Lens Effect as a Power-Limiting Device. *Appl. Phys. Lett.* **1967,** *10* (3), 100-101.
7. Muller, O.; Pichot, V.; Merlat, L.; Spitzer, D., Optical limiting properties of surface functionalized nanodiamonds probed by the Z-scan method. *Sci Rep* **2019,** *9* (1), 519.
8. Mansour, K.; Soileau, M. J.; Stryland, E. W. V., Nonlinear optical properties of carbon-black suspensions (ink). *J. Opt. Soc. Am. B* **1992,** *9* (7), 1100-1109.
9. Vivien, L.; Riehl, D.; Delouis, J.-F.; Delaire, J. A.; Hache, F.; Anglaret, E., Picosecond and nanosecond polychromatic pump?probe studies of bubble growth in carbon-nanotube suspensions. *J. Opt. Soc. Am. B* **2002,** *19* (2), 208-214.
10. Tutt, L. W.; Kost, A., Optical limiting performance of C60 and C70 solutions. *Nature* **1992,** *356* (6366), 225-226.
11. Cha, M.; Sariciftci, N. S.; Heeger, A. J.; Hummelen, J. C.; Wudl, F., Enhanced nonlinear absorption and optical limiting in semiconducting polymer/methanofullerene charge transfer films. *Appl. Phys. Lett.* **1995,** *67* (26), 3850-3852.
12. Sun, Y.-P.; Riggs, J. E.; Liu, B., Optical Limiting Properties of [60]Fullerene Derivatives. *Chem. Mater.* **1997,** *9* (5), 1268-1272.
13. Dini, D.; Barthel, M.; Hanack, M., Phthalocyanines as Active Materials for Optical Limiting. *Eur. J. Org. Chem.* **2001,** *2001* (20), 3759-3769.
14. Four, M.; Riehl, D.; Mongin, O.; Blanchard-Desce, M.; Lawson-Daku, L. M.; Moreau, J.; Chauvin, J.; Delaire, J. A.; Lemercier, G., A novel ruthenium(II) complex for two-photon absorption-based optical power limiting in the near-IR range. *Phys. Chem. Chem. Phys.* **2011,** *13* (38), 17304-12.
15. Zieba, R.; Desroches, C.; Chaput, F.; Carlsson, M.; Eliasson, B.; Lopes, C.; Lindgren, M.; Parola, S., Preparation of Functional Hybrid Glass Material from Platinum (II) Complexes for Broadband Nonlinear Absorption of Light. *Adv. Funct. Mater.* **2009,** *19* (2), 235-241.
16. Su, H.; Zhu, S.; Qu, M.; Liu, R.; Song, G.; Zhu, H., 1,3,5-Triazine-Based Pt(II) Metallogel Material: Synthesis, Photophysical Properties, and Optical Power-Limiting Performance. *J. Phys. Chem. C.* **2019,** *123* (25), 15685-15692.
17. Perry, J. W.; Mansour, K.; Lee, I.-Y. S.; Wu, X.-L.; Bedworth, P. V.; Chen, C.-T.; Ng, D.; Marder, S. R.; Miles, P.; Wada, T.; Tian, M.; Sasabe, H., Organic Optical Limiter with a Strong Nonlinear Absorptive Response. *Science* **1996,** *273* (5281), 1533-1536.
18. Muller, O.; Gibot, P., Optical limiting properties of templated Cr2O3 and WO3 nanoparticles. *Opt. Mater.* **2019,** *95*, 109220.
19. Hu, H.; Przhonska, O. V.; Terenziani, F.; Painelli, A.; Fishman, D.; Ensley, T. R.; Reichert, M.; Webster, S.; Bricks, J. L.; Kachkovski, A. D.; Hagan, D. J.; Van Stryland, E. W., Two-photon absorption spectra of a near-infrared 2-azaazulene polymethine dye: solvation and ground-state symmetry breaking. *Phys. Chem. Chem. Phys.* **2013,** *15* (20), 7666-78.
20. Padilha, L. A.; Webster, S.; Przhonska, O. V.; Hu, H.; Peceli, D.; Ensley, T. R.; Bondar, M. V.; Gerasov, A. O.; Kovtun, Y. P.; Shandura, M. P.; Kachkovski, A. D.; Hagan, D. J.; Stryland, E. W. V., Efficient Two-Photon Absorbing Acceptor-π-Acceptor Polymethine Dyes. *J. Phys. Chem. A* **2010,** *114* (23), 6493-6501.
21. Kurotobi, K.; Kim, K. S.; Noh, S. B.; Kim, D.; Osuka, A., A quadruply azulene-fused porphyrin with intense near-IR absorption and a large two-photon absorption cross section. *Angew. Chem. Int. Ed. Engl.* **2006,** *45* (24), 3944-7.
22. Ahn, T. K.; Kim, K. S.; Kim, D. Y.; Noh, S. B.; Aratani, N.; Ikeda, C.; Osuka, A.; Kim, D., Relationship between Two-Photon Absorption and the π-Conjugation Pathway in Porphyrin Arrays through Dihedral Angle Control. *J. Am. Chem. Soc.* **2006,** *128* (5), 1700-1704.
23. Kamada, K.; Fuku-en, S.-i.; Minamide, S.; Ohta, K.; Kishi, R.; Nakano, M.; Matsuzaki, H.; Okamoto, H.; Higashikawa, H.; Inoue, K.; Kojima, S.; Yamamoto, Y., Impact of Diradical Character on Two-Photon Absorption: Bis(acridine) Dimers Synthesized from an Allenic Precursor. *J. Am. Chem. Soc.* **2013,** *135* (1), 232-241.
24. Ni, Y.; Lee, S.; Son, M.; Aratani, N.; Ishida, M.; Samanta, A.; Yamada, H.; Chang, Y. T.; Furuta, H.; Kim, D.; Wu, J., A Diradical Approach towards BODIPY-Based Dyes with Intense Near-Infrared Absorption around lambda=1100 nm. *Angew. Chem. Int. Ed. Engl.* **2016,** *55* (8), 2815-9.
25. Bouit, P.-A.; Wetzel, G.; Berginc, G.; Loiseaux, B.; Toupet, L.; Feneyrou, P.; Bretonnière, Y.; Kamada, K.; Maury, O.; Andraud, C., Near IR Nonlinear Absorbing Chromophores with Optical Limiting Properties at Telecommunication Wavelengths. *Chem. Mater.* **2007,** *19* (22), 5325-5335.
26. Bouit, P.-A.; Westlund, R.; Feneyrou, P.; Maury, O.; Malkoch, M.; Malmström, E.; Andraud, C., Dendron-decorated cyanine dyes for optical limiting applications in the range of telecommunication wavelengths. *New J. Chem.* **2009,** *33* (5), 964.
27. Hales, J. M.; Cozzuol, M.; Screen, T. E. O.; Anderson, H. L.; Perry, J. W., Metalloporphyrin polymer with temporally agile, broadband nonlinear absorption for optical limiting in the near infrared. *Opt. Express* **2009,** *17* (21), 18478-18488.
28. Bouit, P.-A.; Kamada, K.; Feneyrou, P.; Berginc, G.; Toupet, L.; Maury, O.; Andraud, C., Two-Photon Absorption-Related

Properties of Functionalized BODIPY Dyes in the Infrared Range up to Telecommunication Wavelengths. *Adv. Mater.* **2009,** *21* (10-11), 1151-1154.
29. Pascal, S.; Bellier, Q.; David, S.; Bouit, P.-A.; Chi, S.-H.; Makarov, N. S.; Le Guennic, B.; Chibani, S.; Berginc, G.; Feneyrou, P.; Jacquemin, D.; Perry, J. W.; Maury, O.; Andraud, C., Unraveling the Two-Photon and Excited-State Absorptions of Aza-BODIPY Dyes for Optical Power Limiting in the SWIR Band. *J. Phys. Chem. C* **2019,** *123* (38), 23661-23673.
30. Bellier, Q.; Makarov, N. S.; Bouit, P. A.; Rigaut, S.; Kamada, K.; Feneyrou, P.; Berginc, G.; Maury, O.; Perry, J. W.; Andraud, C., Excited state absorption: a key phenomenon for the improvement of biphotonic based optical limiting at telecommunication wavelengths. *Phys. Chem. Chem. Phys.* **2012,** *14* (44), 15299-307.
31. Parola, S.; Julián-López, B.; Carlos, L. D.; Sanchez, C., Optical Properties of Hybrid Organic-Inorganic Materials and their Applications. *Adv. Funct. Mater.* **2016,** *26* (36), 6506-6544.
32. Château, D.; Bellier, Q.; Chaput, F.; Feneyrou, P.; Berginc, G.; Maury, O.; Andraud, C.; Parola, S., Efficient hybrid materials for optical power limiting at telecommunication wavelengths. *J. Mater. Chem. C* **2014,** *2* (26), 5105.
33. Judeinstein, P.; Sanchez, C., Hybrid organic–inorganic materials: a land of multidisciplinarity. *J. Mater. Chem.* **1996,** *6* (4), 511-525.
34. Desroches, C.; Parola, S.; Cornu, D.; Miele, P.; Baldeck, P. L.; Lopes, C., Sol-gel Nanohybrid Materials Incorporating Functional Thiacalixarenes for Non-Linear Optical Applications. *MRS Proceedings* **2003,** *771*, L7.16.
35. Örtenblad, M.; Parola, S.; Chaput, F.; Desroches, C.; Sigala, C.; Létoffé, J. M.; Miele, P.; Baldeck, P. L.; Eliasson, B.; Eriksson, A.; Lopes, C., Hybrid materials for Optical Limiting. *MRS Proceedings* **2004,** *847*, EE14.3.
36. Tao, L.; Zhou, B.; Bai, G.; Wang, Y.; Yu, S. F.; Lau, S. P.; Tsang, Y. H.; Yao, J.; Xu, D., Fabrication of Covalently Functionalized Graphene Oxide Incorporated Solid-State Hybrid Silica Gel Glasses and Their Improved Nonlinear Optical Response. *J. Phys. Chem. C* **2013,** *117* (44), 23108-23116.
37. Innocenzi, P.; Brusatin, G., Fullerene-Based Organic–Inorganic Nanocomposites and Their Applications. *Chem. Mater.* **2001,** *13* (10), 3126-3139.
38. Westlund, R.; Malmström, E.; Lopes, C.; Öhgren, J.; Rodgers, T.; Saito, Y.; Kawata, S.; Glimsdal, E.; Lindgren, M., Efficient Nonlinear Absorbing Platinum(II) Acetylide Chromophores in Solid PMMA Matrices. *Adv. Funct. Mater.* **2008,** *18* (13), 1939-1948.
39. Gorman, A.; Killoran, J.; O'Shea, C.; Kenna, T.; Gallagher, W. M.; O'Shea, D. F., In Vitro Demonstration of the Heavy-Atom Effect for Photodynamic Therapy. *J. Am. Chem. Soc.* **2004,** *126* (34), 10619-10631.
40. Le Guennic, B.; Jacquemin, D., Taking up the cyanine challenge with quantum tools. *Acc. Chem. Res.* **2015,** *48* (3), 530-7.
41. Pascal, S.; Getmanenko, Y. A.; Zhang, Y.; Davydenko, I.; Ngo, M. H.; Pilet, G.; Redon, S.; Bretonnière, Y.; Maury, O.; Ledoux-Rak, I.; Barlow, S.; Marder, S. R.; Andraud, C., Design of Near-Infrared-Absorbing Unsymmetrical Polymethine Dyes with Large Quadratic Hyperpolarizabilities. *Chem. Mater.* **2018,** *30* (10), 3410-3418.
42. Corredor, C. C.; Belfield, K. D.; Bondar, M. V.; Przhonska, O. V.; Yao, S., One- and two-photon photochemical stability of linear and branched fluorene derivatives. *J. Photoch. Photobio. A* **2006,** *184* (1-2), 105-112.
43. Rosenthal, I., Photochemical stability of rhodamine 6G in solution. *Opt. Commun.* **1978,** *24* (2), 164-166.
44. El-Daly, S. A.; El-Azim, S. A.; Elmekawey, F. M.; Elbaradei, B. Y.; Shama, S. A.; Asiri, A. M., Photophysical parameters, excitation energy transfer, and photoreactivity of 1,4-bis(5-phenyl-2-oxazolyl)benzene (POPOP) laser dye. *Int. J. Photoenergy* **2012,** *2012*, 458126/1-10.
45.Azim, S. A.; Al-Hazmy, S. M.; Ebeid, E. M.; El-Daly, S. A., A new coumarin laser dye 3-(benzothiazol-2-yl)-7-hydroxycoumarin. *Opt. Laser Technol.* **2005,** *37*, 245-249.